

# Hardware Architecture and Algorithm Co-design for Multi-Layer Photonic Neuromorphic Network with Excitable VCSELs-SA

Shuiying Xiang<sup>1,2,\*</sup>, Zhenxing Ren<sup>1</sup>, Yahui Zhang<sup>1</sup>, Xingxing Guo<sup>1</sup>, Ziwei Song<sup>1</sup>, Aijun Wen<sup>1</sup>, Yue Hao<sup>2</sup>

<sup>1</sup> State Key Laboratory of Integrated Service Networks, Xidian University, Xi'an 710071, China

<sup>2</sup> State Key Discipline Laboratory of Wide Bandgap Semiconductor Technology, School of Microelectronics, Xidian University, Xi'an 710071, China.

jxxy@126.com

**Abstract:** We design a multi-layer photonic spiking neural network with excitable VCSELs-SA. Numerical results based on the rate-equation models show that the proposed neuromorphic network architecture is capable of solving the classical XOR problem by supervised-learning. © 2020 The Author(s)

**OCIS codes:** (200.4700) Optical neural systems; (140.7260) Vertical cavity surface emitting lasers.

## 1. Introduction

The electronic neuromorphic computing system has been extensively demonstrated based on complementary metal oxide semiconductor (CMOS) and the emerging memories [1-3]. As an alternative, the photonic platform has gained increasing attention for hardware neuromorphic computing, due to the fascinating advantages such as high speed, wide bandwidth, and massive parallelism [4-13]. In 2017, a new architecture for a fully optical neural network in a silicon photonic integrated circuit was demonstrated, which offered enhancement in computational speed and power efficiency [7]. In 2019, an all-optical spiking neural network (SNN) consisting of four neurons and sixty synapses based on phase-change materials was implemented on a nanophotonic chip [9]. Nahmias et al. developed an analytical model for photonic neuron based on the vertical-cavity surface-emitting laser with an embedding saturable (VCSEL-SA) [5]. It is well-known that the inhibitory synapse is usually required to realize the nonlinear separable problem such as the XOR task. Note, the inhibition is difficult to realize in the optical domain as there is no negative optical pulse. Very recently, we proposed to emulate the inhibitory dynamics based on the two modes VCSEL-SA subject to dual-polarized optical injection [10]. We further developed a computational model of all-optical SNN for unsupervised learning, by incorporating the plasticity model based on a vertical-cavity semiconductor amplifier (VCSOA) [11]. However, a computing primitive and computational model for multi-layer photonic SNN consisting of excitable VCSELs-SA is still lack, and the hardware-friendly learning algorithm for multi-layer photonic SNN has not yet been addressed.

In this work, we propose a hardware architecture and derive the system-level self-consistent model for a multi-layer photonic SNN. VCSEL-SA and VCSOA are employed as photonic neurons and synapse, due to the advantages of low cost, low power consumption, and easy implementation of integration. Furthermore, a specific supervised learning algorithm, by the combination of the STDP rule and Tempotron rule, is developed for the proposed multi-layer photonic SNN, taking advantage of the inhibitory dynamics of VCSEL-SA. The classical XOR problem based on the modeling-based photonic SNN is successfully realized.

## 2. Hardware Architecture and Algorithm Co-design of proposed multi-layer photonic SNN

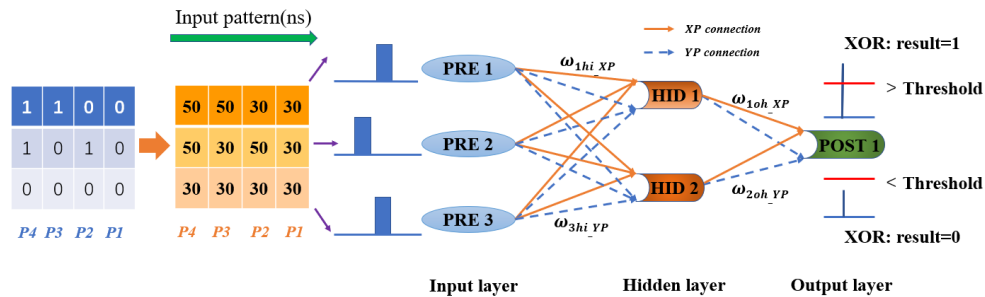


Fig. 1. The architecture of the proposed multi-layer photonic SNN for solving the XOR task.

To solve the nonlinear classification problem, we designed a multi-layer photonic SNN based on the excitable VCSEL-SA, as shown in Fig.1. Here, 00 (P1), 01 (P2), 10 (P3), 11 (P4) are four input patterns. A bias (0) is added for

each pattern. The bit 0 (1) is pre-encoded as a rectangle pulse with central timing at 30ns (50ns). The rectangle pulses are then injected into the x-polarization (XP) mode of three VCSEL-SA (i.e., PREs), respectively, to implement spike encoding. The XP output of the input layer is then injected into both the XP and y-polarization (YP) modes of two VCSEL-SA in the hidden layer. Similarly, the XP output of the hidden layer is then propagated to both the XP and YP mode of the VCSEL-SA in the output layer. The target is pre-defined as follows. For the input patterns P1 and P4, the XOR result is 0, and the POST emits no spike. While for the input patterns P2 and P3, the XOR result is 1, the POST is allowed to emit spikes.

Here, the theoretical model of photonic neuron is based on the combination of Yamada model and spin-flip model for a VCSEL-SA with two polarization-resolved modes [5, 10-11]:

$$\frac{dF_{ix,hx,ox}}{dt} = \frac{1}{2}(1+i\alpha)[(D_1 + D_2 - 1)F_{ix,hx,ox} + i(d_1 + d_2)F_{iy,hy,oy}] - (\varepsilon_a + i\varepsilon_p)F_{ix,hx,ox} + k_{ix}F_{inix}(t)e^{i2\pi f_{ix}t} + \omega_{hix,ohx}F_{ix,hx}(t)e^{i2\pi f_{hi,oh}t} \quad (1)$$

$$\frac{dF_{iy,hy,oy}}{dt} = \frac{1}{2}(1+i\alpha)[(D_1 + D_2 - 1)F_{iy,hy,oy} - i(d_1 + d_2)F_{ix,hx,ox}] + (\varepsilon_a + i\varepsilon_p)F_{iy,hy,oy} + \omega_{hiy,ohy}F_{ix,hx}(t)e^{i2\pi f_{hi,oh}t} \quad (2)$$

$$\dot{D}_{1,2} = \gamma_{1,2}[\mu_{1,2} - D_{1,2} - \frac{1}{2}a_{1,2}(D_{1,2} + d_{1,2})|F_{ix,hx,ox} - iF_{iy,hy,oy}|^2 - \frac{1}{2}a_{1,2}(D_{1,2} - d_{1,2})|F_{ix,hx,ox} + iF_{iy,hy,oy}|^2 + c_{12,21}D_{2,1}] \quad (3)$$

$$\dot{d}_{1,2} = -\gamma_{s1,2}d_{1,2} - \gamma_{1,2}[\frac{1}{2}a_{1,2}(D_{1,2} + d_{1,2})|F_{ix,hx,ox} - iF_{iy,hy,oy}|^2 - \frac{1}{2}a_{1,2}(D_{1,2} - d_{1,2})|F_{ix,hx,ox} + iF_{iy,hy,oy}|^2 - c_{12,21}d_{2,1}] \quad (4)$$

Where subscripts  $i, h, o$  denote VCSEL-SA in the input, hidden and output layer, respectively. The third term in Eq.(1) represents the external stimulation for the XP mode and exists only for the input layer, where  $F_{inix}(t)$  is the external stimulating rectangle pulse and  $k_{ix}=0.5$  is the stimuli strength. The last term in Eq. (1) (Eq. (2)) denotes the injection for the XP (YP) mode for the hidden and output layer, respectively. The initial value of  $\omega_{hix,ohx}$ ,  $\omega_{hiy,ohy}$  is a random value ranging from 0 to 0.2. Other parameters and their values are chosen according to those in [10].

The synapse weight  $\omega_{hix,ohx}$  and  $\omega_{hiy,ohy}$  can be adjusted by repeatedly feeding the input patterns to the photonic SNN with supervised learning algorithm. In our proposed multi-layer photonic SNN, a specific hardware-friendly algorithm is required to adjust the weight for both the XP connection (from XP to XP) and the YP connection (from XP to YP). To this end, we design a supervised learning algorithm by modifying the Tempotron rule and the photonic STDP rule [11, 14-15]. The weight update amount  $\Delta\omega_{hix}$  ( $\Delta\omega_{ohx}$ ) between the XP mode of input and hidden (hidden and output) layers can be calculated as follows,

$$\Delta\omega_{hix,ohx} = \begin{cases} +\omega_f \cdot \Delta\omega_{STDP}(\Delta t_{hi,oh}), & \text{if } n^d = 1, n^o = 0 \text{ and } \Delta t_{hi,oh} > 0 \\ -\omega_f \cdot \Delta\omega_{STDP}(\Delta t_{hi,oh}), & \text{if } n^d = 0, n^o = 1 \text{ and } \Delta t_{hi,oh} > 0 \end{cases} \quad (5)$$

Where  $\Delta t_{hi} = t_h - t_i$ ,  $\Delta t_{oh} = t_o - t_h$ ,  $t_i$ ,  $t_h$  and  $t_o$  denote the spike timing in the input, hidden and output layer, respectively.  $\Delta\omega_{STDP}(\Delta t_{hi,oh})$  is employed as in [11].  $n^d=1$  ( $n^o=1$ ) represents the target output (actual output) with spike emission, and  $n^d=0$  ( $n^o=0$ ) indicates target output (actual output) without spike emission. When  $n^d=n^o$ ,  $\Delta\omega_{hix,ohx}=0$ .  $\omega_f=0.01$  is learning rate. Between a given pair of two layers, the weight update amount of the YP mode is the same as that for the XP mode, but the weight update sign is opposite. Namely,  $\omega_{hix,ohx\_new} = \omega_{hix,ohx\_old} + \Delta\omega_{hix,ohx}$  and  $\omega_{hiy,ohy\_new} = \omega_{hiy,ohy\_old} - \Delta\omega_{hiy,ohy}$ .

### 3. Numerical Results

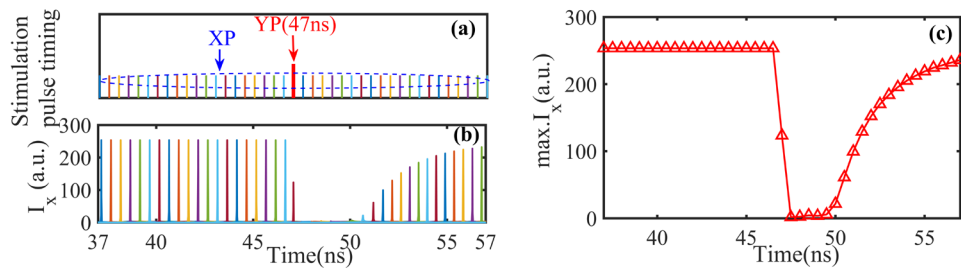


Fig.2. The inhibitory dynamics of VCSEL-SA subject to dual-polarized optical injection. (a) The external stimulation pulse timing for the XP mode and YP mode, (b) the response in the XP mode with  $I_x = |F_x|^2$ , (c) the peak intensity corresponding to (b).

At first, the inhibitory dynamics of the VCSEL-SA subject to dual-polarized optical injection is presented in Fig.2. Here, the external stimulation pulse for the YP mode is fixed at  $t_y=47\text{ns}$ , while the stimulation pulse for XP mode is varied from  $t_x=37\text{ns}$  to  $t_x=57\text{ns}$ . It can be seen that, when  $t_x < t_y$ , the response in the XP mode is not affected by the stimulation pulse in the YP mode, and reaches its maximum. On the other hand, when  $t_x > t_y$ , the response dynamics is quite different. Within the range  $48\text{ns} < t_x < 50\text{ns}$ , the response in the XP mode is significantly inhibited, the output intensity is very small, as the carrier numbers is reduced substantially due to the stimulation injection in the YP mode. After that, the peak intensity of XP response spike is increased gradually due to the carrier recovery.

Next, the training process for the four different patterns is presneted in Fig.3 (a). It can be seen that, with the designed supervised learning algorithm to adjust the synpatic weight for both XP and YP connection, the targets for all the patterns are achieved after several training epochs. The evolution of the weight during traning is also presented in Figs.3(b) and (c). With these trained weight matrix, when the input pattern is P1 or P4, the POST emits no spike in the XP mode, while for the patterns P2 and P3, the POST emits spike in the XP mode. Thus, the proposed hardware architecture and algorithm for multi-layer photonic SNN is capable of sovling the XOR task.

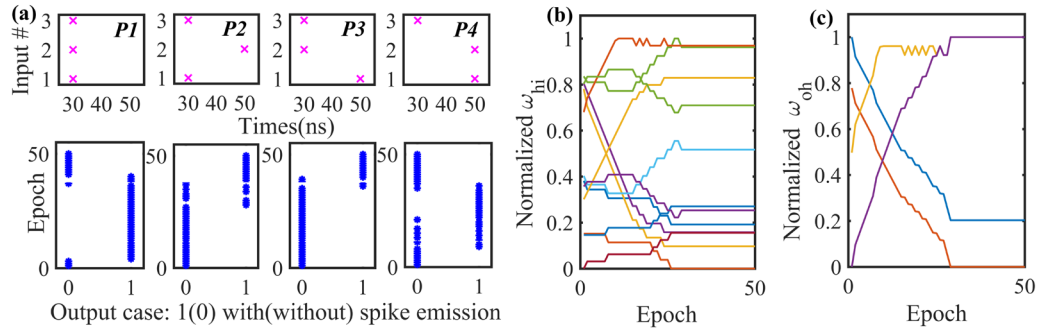


Fig.3. Training process for the XOR task. (a) The output of the POST for four patterns, 0 (1) represents without (with) spike emission, (b) the evolution of weight between the input and hidden layers, (c) the evolution of weight between the hidden and output layers.

#### 4. Conclusions

We proposed a framework for the hardware architecture and learning algorithm co-design for a multi-layer photonic SNN consisting of excitable VCSEL-SA with two polarization-resolved modes. By designing specific hardware-friendly supervised learning algorithm based on the photonic STDP rule, the proposed photonic SNN is capable of solving the XOR task.

#### 5. References

- [1] M. Prezioso, et al, "Training and operation of an integrated neuromorphic network based on metal-oxide memristors," *Nature*, 521, 61–64 (2015).
- [2] R. A. Nawrocki, R. M. Voyles and S. E. Shaheen, "A mini review of neuromorphic architectures and implementations," *IEEE T. Electron Dev.*, 63, 3819-3829 (2016).
- [3] J. Pei, et al, "Towards artificial general intelligence with hybrid Tianjic chip architecture," *Nature*, 572, 106–111 (2019).
- [4] A. Hurtado, K. Schires, I. Henning, and M. Adams, "Investigation of vertical cavity surface emitting laser dynamics for neuromorphic photonic systems," *Appl. Phys. Lett.*, 100, 103703-103703 (2012).
- [5] M. A. Nahmias, B. J. Shastri, A. N. Tait, and P. R. Prucnal, "A leaky integrate-and-fire laser neuron for ultrafast cognitive computing," *IEEE J. Sel. Top. Quantum Electron.*, 19, 1800212 (2013).
- [6] P. R. Prucnal, et al, "Recent progress in semiconductor excitable lasers for photonic spike processing," *Adv. Opt. Photon.*, 8, 228-299 (2016).
- [7] Y. Shen, et al., "Deep learning with coherent nanophotonic circuits," *Nat. Photon.*, 11, 441-447 (2017).
- [8] T. Deng, J. Robertson, and A. Hurtado, "Controlled propagation of spiking dynamics in vertical-cavity surface-emitting lasers: towards neuromorphic photonic networks," *IEEE J. Sel. Top. Quantum Electron.*, 23, 1800408 (2017).
- [9] J. Feldmann, N. Youngblood, C. D. Wright, H. Bhaskaran & W. H. P. Pernice, "All-optical spiking neurosynaptic networks with self-learning capabilities," *Nature*, 569, 208-215 (2019).
- [10] Y. Zhang, S. Y. Xiang, X. Guo, A. Wen, and Y. Hao, "All-optical inhibitory dynamics in photonic neuron based on polarization mode competition in a VCSEL with an embedded saturable absorber," *Opt. Lett.*, 44, 1548-1551 (2019).
- [11] S. Y. Xiang, Y. Zhang, J. Gong, X. Guo, L. Lin and Y. Hao, "STDP-based unsupervised spike pattern learning in a photonic spiking neural network with VCSELs and VCSOs," *IEEE J. Sel. Top. Quantum Electron.*, 25, 1700109 (2019).
- [12] J. Robertson, E. Wade, Y. Kopp, J. Bueno, and A. Hurtado, "Toward neuromorphic photonic networks of ultrafast spiking laser neurons," *IEEE J. Sel. Top. Quantum Electron.*, 26, 7700715 (2020).
- [13] H.-T. Peng, et al., "Temporal information processing with an integrated laser neuron," *IEEE J. Sel. Top. Quantum Electron.*, 26, 5100209 (2020).
- [14] G. Bi and M. Poo, "Synaptic modifications in cultured hippocampal neurons: Dependence on spike timing, synaptic strength, and postsynaptic cell type," *J. Neurosci.*, 18, 10464-10472 (1998).
- [15] R. Güttig and H. Sompolinsky, "The tempotron: A neuron that learns spike timing-based decisions," *Nat. Neurosci.*, 9, 420–428 (2006).